Chapter 12
Ultrasound

James R. Costello, Hina Arif, Bobby Kalb, and Diego R. Martin

Contents

12.1 Introduction

Over the past few decades, there has been a driving push in medical imaging to develop techniques that are noninvasive and without exposure to potentially harmful ionizing radiation. The two imaging modalities that are leading this initiative are ultrasound and magnetic resonance imaging (MRI).

J.R. Costello, MD, PhD (✉)
Department of Medical Imaging, University of Arizona, 1501 North Campbell Ave, P.O. Box 245067, Tucson, AZ 85725, USA

Radiology Associates of Macon, PC, 770 Pine Street, Macon, GA 31201, USA
e-mail: jcostello@radiology.arizona.edu

H. Arif, MD • B. Kalb, MD • D.R. Martin, MD, PhD, FRCPC
Department of Medical Imaging, University of Arizona, 1501 North Campbell Ave, P.O. Box 245067, Tucson, AZ 85725, USA
e-mail: hinaarif@radiology.arizona.edu; bkalb@radiology.arizona.edu; dmartin@radiology.arizona.edu

M. Maqbool (ed.), *An Introduction to Medical Physics*, Biological and Medical Physics, Biomedical Engineering, DOI 10.1007/978-3-319-61540-0_12

Ultrasound generates images through the interaction of the body with sound waves. Through differences in the interaction of tissue with incident, high-frequency sound waves, two-dimensional (2D) grayscale images of the body can be generated. Additionally, ultrasound can measure blood flow and velocity, provide multiplanar and three-dimensional (3D) imaging, visualize dynamic moving structures such as a fetus and the heart, and evaluate superficial structures such as the thyroid and joints with high-resolution imaging. All of these imaging features are provided by hardware which is portable and easy to transport, unlike the bulky stationary scanners of computed tomography and MRI. Additionally, ultrasound represents a cost-effective examination that can be repeated on regular intervals but without the significant cost burden of other imaging exams.

The origins of ultrasound imaging began well over 200 years ago. In the late 1700s Lazzaro Spallanzani identified that bats used a sensory tracking system other than sight to navigate. Spallanzani detailed this process as echolocation or spatial navigation through the emission and detection of inaudible sound. In 1826 Jean-Daniel Colladon introduced the underwater church bell as the first ultrasound transducer. With this first instrument, Colladon proved that the speed of sound traveled faster in water than in air. In 1880 Pierre and Jacques Curie described the piezoelectric effect and how electricity can be generated within a quartz crystal when mechanically vibrated. Acoustic energy potentially serves as a source for such mechanical vibration. This idea serves as the operating principle for the modern-day medical ultrasound transducer.

During World War I and II, military sonar research helped advance the field of ultrasound. In 1915 Paul Langevin constructed the hydrophone to help ships detect icebergs and to locate underwater submarines. In 1937 Sergei Sokolov described the "Sokolov tube" for underwater imaging. This device advanced the field of underwater sonography and introduced the first real-time sonar display. From these developments in military sonar research, applications in medical imaging would soon arise. In 1942 Dr. Karl Dussik described the application of ultrasound to visualize the mass effect of brain tumors and the resulting effect upon the cerebral ventricles. Later in 1948 George Ludwig and Francis Struthers detailed the application of ultrasound for imaging of gallstones which was later followed by Dr. Ian Donald's use of ultrasound in obstetric imaging to measure the parietal diameter of the fetal head. All of this work materialized in 1963 with the introduction of the first commercial ultrasound scanner (Kremkau 1998; Goldstein 1993; Hendrick et al. 1995; Zagzebski 1996; Bushberg et al. 2002).

Within this chapter, we will discuss the physics of sound, transducer design and optimization, the generation of an ultrasound image, artifacts of ultrasound imaging, and Doppler imaging. Through this discussion, we hope the reader acquires an understanding of the current applications of ultrasound and the promise for this technique's continued maturation within medical imaging.

12.2 Contrast Versus Resolution

Fundamental to a discussion of medical imaging is differentiating between the properties of image contrast versus image resolution. Image contrast distinguishes an object of interest from the surrounding background tissue that contains it. For example, contrast refers to the ability of ultrasound to distinguish a hepatic mass such as a hepatocellular carcinoma, a type of liver cancer, from the background liver parenchyma which surrounds the mass. Image resolution reflects the ability of an imaging system to resolve two adjacent structures of interest from each other. For example, an ultrasound image with sufficient spatial resolution can distinguish two adjacent hepatic masses as opposed to a lower-resolution image which displays a single lobulated mass with no demarcation where one mass ends and the other begins as shown in Fig. 12.1.

12.3 Acoustic Theory

Ultrasound generates medical images through the interaction of sound with different tissue types. Sound represents mechanical energy that travels through an elastic medium (air, water, tissue) as a longitudinal wave with an alternating sequence of compression and rarefaction of its constituent particles. Rarefaction is defined as a decrease in the density of the medium or the opposite effect of compression (Bigelow et al. 2011). Compression of the elastic medium is represented by positive displacement of the wave's pressure amplitude, while rarefaction closely follows the compressive event with a mirrored response of negative displacement of the

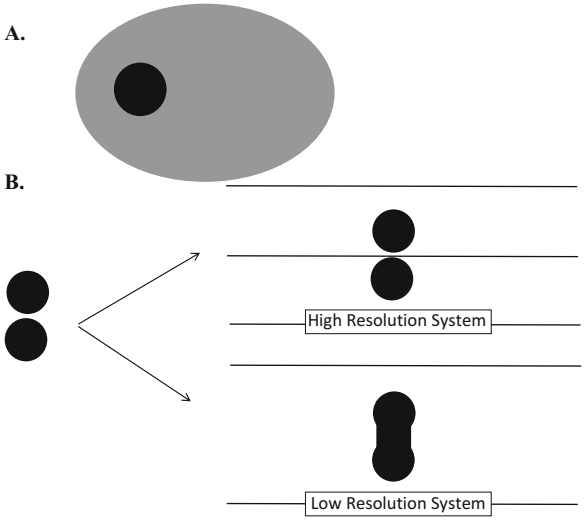

Fig. 12.1 *Image contrast versus image resolution*. (**a**) Contrast: a high-contrast imaging system can resolve the *black* ball from the background *gray* area. (**b**) A high-resolution system can distinguish the two *black* balls from each other, whereas the low-resolution system volume averages the two *black* balls into one imaged *black* object

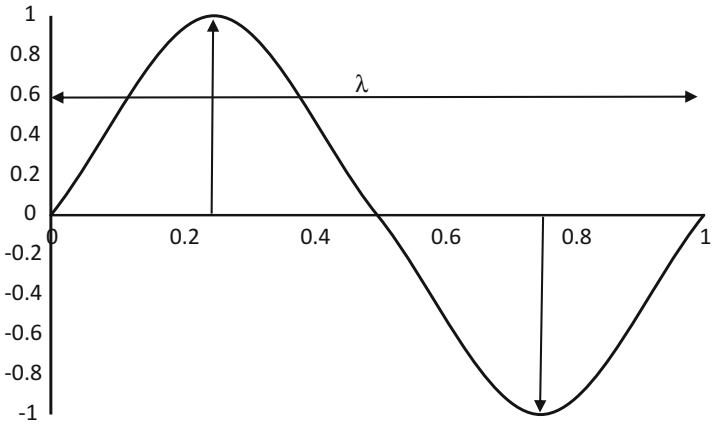

Fig. 12.2 *Pressure wave*. Ultrasound represents a traveling wave of mechanical energy with alternating compression and rarefaction of the elastic medium

wave's pressure amplitude. Through this repetitive cycle, mechanical energy or sound is transported through the elastic medium as shown in Fig. 12.2.

12.3.1 Properties of Sound

The wavelength of sound, λ (meters), is defined as the distance between successive compressive peaks, while the frequency of sound, f, reflects the number of times that the wave cycle repeats per second. Frequency is measured in cycles per second or Hertz. Human hearing falls within a frequency range of 20 Hertz (Hz)–20 kilohertz (kHz). Ultrasound transmission occurs at a frequency range above the upper limit of human hearing. For medical imaging, this range is defined between 1 and 20 megahertz (MHz). The period of the wave, T (seconds), represents the time between successive compressive peaks or the reciprocal of the frequency. The speed of sound, c (meters/second), reflects the distance traveled by the wave over the length of time needed to complete 1 cycle which can also be expressed as:

$c = \lambda/T$

or

$$c = \lambda^* f \tag{12.1}$$

If sound is traveling within muscle with a speed of 1585 m/sec and a frequency of 3 MHz, then the wavelength will be equal to 0.528 mm.

The speed of sound varies depending on the properties of the elastic medium.

$$c = \sqrt{\beta/\rho} \tag{12.2}$$

β (kilogram/meter) represents the bulk modulus which reflects the stiffness of the elastic medium, while ρ (kilogram/meter^3) represents the density of the elastic medium. For a compressible medium such as gas, the speed of sound will be slower in comparison to a less compressible medium such as metal or calcified bone. Additionally, a less dense medium such as dry air will demonstrate a faster speed of sound than a denser medium such as humid air. For reference, the speed of sound in air is 330 m/sec, in soft tissue is 1540 m/sec, and in fatty tissue is 1450 m/sec. As the mechanical sound energy travels between elastic mediums with different speeds of sound, the frequency remains constant, while the wavelength either contracts or expands.

Why is the frequency and wavelength of the transmitted acoustic energy important for ultrasound? As the frequency increases, the wavelength decreases. With a smaller wavelength, the ultrasound possesses greater axial spatial resolution to distinguish between two adjacent structures along the line of transmission or the ultrasound pulse beam. Frequently in medical imaging, an improvement in one imaging parameter comes at a sacrifice to another imaging parameter. With an increase in frequency, the sound energy is attenuated faster, and the depth of penetration for the ultrasound to provide imaging is reduced. With these parameters in mind, high-frequency probes (7.5 MHz–10 MHz) are used to image superficial structures such as the thyroid and musculoskeletal tissue where increased resolution is needed for improved diagnosis. Lower-frequency probes (3.0 MHz–5.0 MHz) are used to image the abdomen where structures are deeper and greater acoustic penetration is needed.

12.3.1.1 The Decibel Scale

When sound travels through an elastic medium, particles vibrate with variations in pressure amplitude reflected by the wave displacement of compression and rarefaction. The intensity of sound reflects the transmitted power per unit area and is roughly equivalent to the square of the pressure amplitude.

$$\text{Intensity} \sim (\text{Pressure})^2 \tag{12.3}$$

As the pressure amplitude doubles, the absolute intensity value increases by four times. The units of absolute intensity level are watts/m^2. Relative sound intensity is measured on the logarithmic scale with decibels (dB) where

$$\text{Relative Intensity (dB)} = 10 \log_{10} \frac{I}{I_o} \tag{12.4}$$

I is the newly measured intensity, while I_o is the original signal intensity which functions as a reference. A change of 10 dB is reflected by a tenfold increase in intensity, while a change of 3 dB is signified by a two-time increase in intensity. A decrease in intensity is shown by a negative decibel value. For example, a reduction

in intensity by 50% equals a change of −3 dB, while a reduction in intensity by 90% relates to a change of −10 dB.

12.3.2 The Dynamics of Sound Interaction

Ultrasound generates images through the interaction of sound with tissue of differing acoustic properties. This interaction is largely governed by the acoustic impedance, *Z*, of the tissue. Acoustic impedance is defined as the product of the density, ρ (kg/m^3), and the speed of sound, c, in the elastic medium.

$$Z = \rho^* c \tag{12.5}$$

The units of acoustic impedance are the Rayl (kg/m^2/sec). The acoustic impedance of air is 0.0004 Rayl, muscle is 1.70 Rayl, and bone is 7.8 Rayl.

When sound travels through the body and encounters an interface with an acoustic impedance mismatch, four different interactions can occur: reflection, refraction, absorption, or scatter.

12.3.2.1 Reflection

Reflected ultrasound energy is critical to the generation of an ultrasound image. The reflected ultrasound energy is called an echo (Fig. 12.3). Reflection occurs at tissue interfaces where there is a difference in the acoustic impedance.

A larger acoustic impedance mismatch results in a larger percentage of the incident energy being reflected. Assuming an angle of incidence from elastic

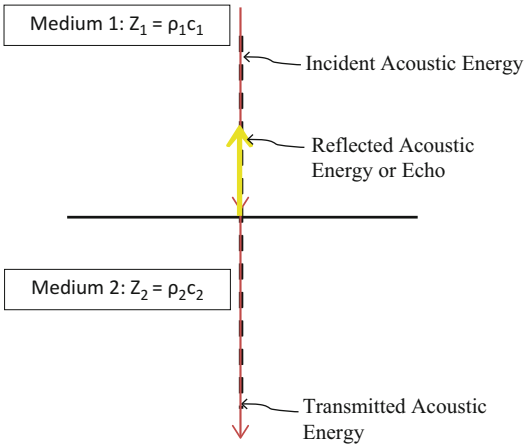

Fig. 12.3 *Reflection of sound with perpendicular incidence to a boundary layer*. At a boundary layer with a difference in acoustic impedance between two mediums and perpendicular incidence (90°) of the incident acoustic energy, a portion of the beam is reflected back to the source, and a portion is transmitted into medium 2

medium 1 perpendicular (90°) to the interface with elastic medium 2, the percentage of incident ultrasound intensity reflected is equal to R_I.

$$R_I = \frac{(Z_2 - Z_1)^2}{(Z_2 + Z_1)} \tag{12.6}$$

Since the percentage of energy reflected plus the energy transmitted must equal 1, the percentage of incident ultrasound intensity transmitted is equal to R_T.

$$R_T = 1 - R_I$$

or

$$R_T = \frac{4Z_1Z_2}{(Z_1 + Z_2)^2} \tag{12.7}$$

For a liver to fat interface, Z_{fat} equals 1.38 Rayl, and Z_{liver} equals 1.65 Rayl. The R_I equals 0.0086 and the R_T equals 0.9914. Given an incident intensity of 50 mW/cm^2, the incident intensity reflected equals 0.43 mW/cm^2, while the incident intensity transmitted equals 49.57 mW/cm^2. Between an air and soft tissue interface, the incident ultrasound energy is near completely reflected. This interaction leads to the generation of a mirror image artifact which will be discussed later. The dynamics of this scenario becomes clear when inputting the low acoustic impedance of air (0.004 Rayl) into the R_T or Eq. (12.7). With the numerator approaching zero, very little acoustic energy is transmitted but rather near completely reflected. To help minimize this effect, acoustic coupling gel or ultrasound jelly is applied between the transducer and the underlying skin.

Other factors that impact reflection include the interface surface characteristics, the size of the interface, and the angle of incidence. The angle of reflection for the echo is equal to the angle of incidence. With an increase in the angle of incidence, the likelihood of the echo being detected by the receiving transducer decreases. Specifically, if the angle of incidence exceeds 3° from the perpendicular interface, a reflected echo is not detected by the ultrasound transducer (Ziskin 1993).

12.3.2.2 Refraction

Refraction describes the change in direction of a transmitted ultrasound beam when the incident ultrasound beam is not orthogonal to the tissue interface, and there is a difference in the speed of sound between the two elastic mediums. In optics this is observed by the redirection of the transmitted light following its passage through a lens. With the difference in the velocity of sound between the two mediums, the frequency of the transmitted pulse will remain constant, but the wavelength will vary in size. The angle of refraction is determined by Snell's law where Θ_t is the

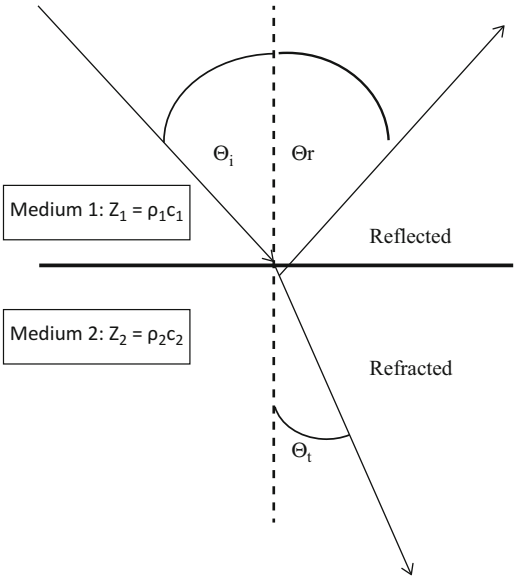

Fig. 12.4 *Reflection and refraction.* Reflection and refraction of acoustic energy occurs at a tissue boundary interface where there is a difference in acoustic impedance (Z) between medium 1 and medium 2. When the incident ultrasound beam is directed toward the boundary interface with nonperpendicular incidence, the reflected echo demonstrates a Θ_r which is equal to Θ_i. The transmitted beam is refracted, and Θ_t or the angel of refraction is defined by Snell's law

angle of refraction, Θ_i is the angle of incidence, and c_1 and c_2 are the respective speed of sounds in mediums 1 and 2 (Fig. 12.4).

$$\frac{\text{Sin}\,(\Theta_t)}{\text{Sin}\,(\Theta_i)} = \frac{c_2}{c_1} \tag{12.8}$$

Diagnostically, refraction is important for it can result in spurious localization of an object of interest through duplication of deeper imaged structures (this is the refraction artifact which will be discussed later). This dynamic is observed frequently at fat/soft tissue interfaces. The speed of sound in fat is 1450 m/sec, while the speed of sound in soft tissue is about 1540 m/sec. This refraction artifact is frequently observed in imaging of the kidneys which are surrounded by prominent retroperitoneal fat.

There is no refraction of sound when $\Theta_i = 90^\circ$ (Fig. 12.3) or c_1 is equal to c_2. Total reflection occurs when c_2 exceeds c_1, and Θ_i is greater than the critical angle (Θ_c). When total reflection occurs, Θ_t equals 90°, and the refracted beam does not travel into medium 2, but rather it runs parallel along the boundary. The critical angle is defined by:

$$\sin\,(\Theta_c) = \frac{c_1}{c_2} \tag{12.9}$$

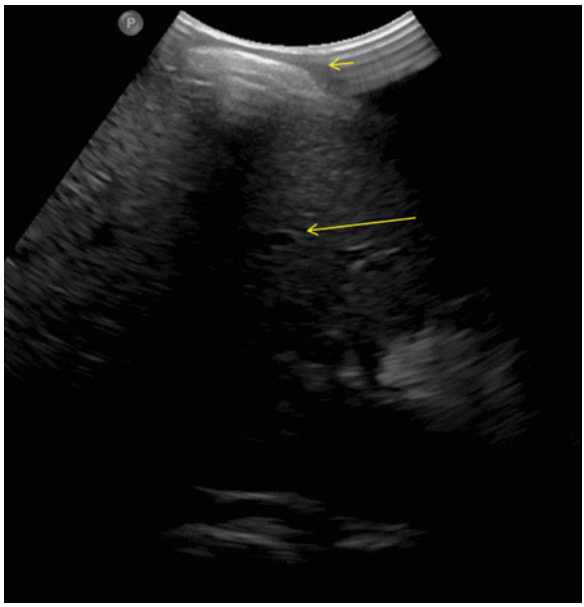

Fig. 12.5 *Absorption*. The ultrasound beam is absorbed by the overlying rib or bone (*small arrow*) and converted into thermal energy. No acoustic energy is transmitted posteriorly, resulting in the clean shadow (*long arrow*)

If sound is traveling from subcutaneous fat ($c_1 = 1.38$ Rayl) into muscle ($c_2 = 1.70$ Rayl), total reflection will occur if the angle of incidence (Θ_i) exceeds the critical angle (Θ_c) of 54.3°.

12.3.2.3 Absorption

Absorption arises when sound energy is lost and converted by a boundary interface from resonating mechanical energy into thermal energy or heat. Absorption occurs more frequently in soft tissue than in fluid, and it happens far more often with bone than with soft tissue. With the loss of sound energy, there is failure to transmit sound beyond the interface of absorption, leading to a posteriorly projecting area devoid of echoes or shadowing. An example of sound energy absorption occurs when an ultrasound beam interacts with an extremely dense tissue such as bone. Posterior to the bone only a clean projecting shadow is visualized (Fig. 12.5).

12.3.2.4 Scatter

Scatter occurs when sound energy interacts with a boundary interface where there is nonspecular reflection. Nonspecular reflection occurs when sound energy interacts with a "rough" surface where the encountered objects are about the same size or smaller than the wavelength of the incident sound. An example would be sound energy interacting with the hepatic parenchyma or tissue of the liver. The liver

contains multiple soft tissue interfaces which are smaller than the wavelength of the incident sound which results in scatter. In contrast, a specular reflector has a smooth surface where the encountered objects at the interface have dimensions much larger than the wavelength of the incident ultrasound energy. Specular reflectors result in reflection and refraction as earlier discussed (Figs. 12.3 and 12.4). If the specular reflector is oriented at 90° to the incident sound, a stronger reflected echo will be generated than if the specular reflector is oriented off-axis from 90°.

When scatter occurs, sound energy is redirected in multiple directions, resulting in weaker echoes with smaller pressure amplitudes returning to the ultrasound probe. While this interaction may seem undesired, scatter actually provides important information about the imaged tissue. Since most tissue types have different cell composition and anatomical structure, a unique scatter "pattern" is generated by how these various organs and tissue interact with ultrasound. This unique "pattern" helps to provide much of the useful diagnostic information within an ultrasound image. Differences in scatter amplitude between regions of an imaged tissue will show as different levels of brightness or echogenicity on the displayed image. Echoes with higher scatter amplitude will be hyperechoic or bright, while echoes with lower scatter amplitude will be hypoechoic or darker. The amplitude of the scattered echo will vary based upon the scatter density (or the extent of scatter per unit volume of tissue), the difference in acoustic impedance at the tissue interface, and the frequency of the ultrasound pulse.

With increases in the frequency of transmitted sound, the wavelength will decrease which will increase the acoustic scatter. With a smaller wavelength, the sound is now able to distinguish some of the small surface irregularities which were indistinguishable with the larger wavelength or smaller frequency transmission. With the tissue interface now appearing "rougher," more acoustic scatter will occur.

Large differences in acoustic impedance are reflected by changes in the speed of sound. With a change in the speed of sound, the transmitted frequency will remain constant, but the wavelength will vary in size. As just described, this change in wavelength will affect the extent of scatter. Unlike specular reflectors which lead to reflection, scatter from nonspecular reflectors are not as significantly impacted by beam direction or angle of incidence (Θ_i) of the ultrasound transducer. When scatter occurs, diffuse echoes are generated unlike the focused and directed echo of reflection.

Through the interactions of reflection, refraction, absorption, and scatter, diagnostic medical images can be generated by an ultrasound machine. A discussion of a representative image of the abdomen best describes these interactions (Fig. 12.6). In the first image, a calcified stone is observed within the gallbladder. The gallbladder is an organ along the undersurface of the gallbladder which stores bile. The calcified stone absorbs the majority of the incident ultrasound energy, resulting in posterior shadowing. The posterior wall of the gallbladder is a specular reflector, and since it is perpendicular to the ultrasound beam, reflection occurs with a bright or hyperechoic wall. The gallbladder lumen is black or anechoic, illustrating through transmission of sound with little or no reflection. The parenchyma of the surrounding liver is intermediate and mixed in echogenicity, indicative of multiple boundary interfaces resulting in scatter.

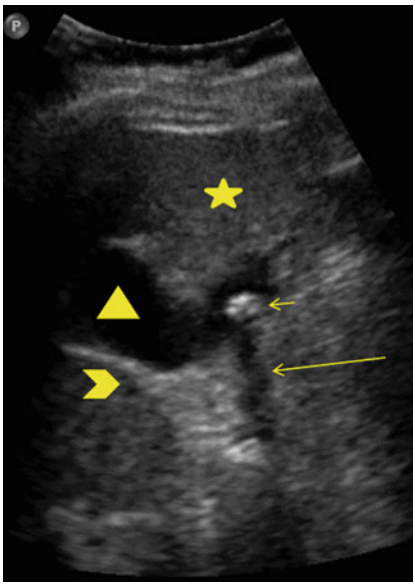

Fig. 12.6 *Acoustic interaction resulting in generation of an ultrasound image*. This is an ultrasound image of the liver and gallbladder. The *star* is in the center of the liver. Scatter of ultrasound energy occurs within the liver, leading to the generation of its unique imaging pattern. The *triangle* is in the center of the gallbladder. The gallbladder contains bile or fluid which neither leads to reflection, absorption, scatter, or reflection. As a result, the sound energy passes through the gallbladder, and its lumen appears dark or anechoic. The *short arrow* is the calcified gallstone. The calcified gallstone absorbs the incident ultrasound energy. Since it absorbs the energy, no ultrasound pulse travels behind the gallstone, resulting in the posterior acoustic shadow, the *long arrow*. The *chevron* illustrates the echogenic posterior wall of the gallbladder where reflection of ultrasound energy occurs

12.3.2.5 Attenuation

As ultrasound energy travels through tissue, the strength of the acoustic energy attenuates or weakens through scatter and absorption. The rate of attenuation of the ultrasound energy will vary depending on the tissue type. For soft tissue, the attenuation coefficient can be generally estimated as:

$$\mu(\text{soft tissue})(\text{dB}) \sim 0.5 * x * f \tag{12.10}$$

The attenuation of sound increases with both distance traveled from the ultrasound probe and increasing frequency. For soft tissue, the attenuation is near linearly proportional to frequency, while for water and bone, the attenuation changes by the frequency squared. Given this relation and when imaging a deep structure such as the pancreas within the abdomen (Fig. 12.7a), a transducer with lower frequency (3–5 MHZ) provides optimal images. When imaging a more superficial structure such as the thyroid gland within the neck (Fig. 12.7b), a higher-frequency transducer (7.5–10 MHz) is used.

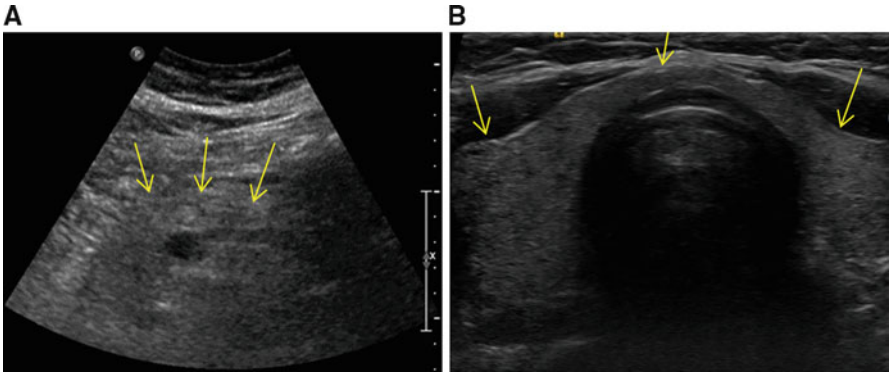

Fig. 12.7 *Ultrasound images using a low-frequency transducer and a high-frequency transducer*. (**a**) Ultrasound image of the pancreas using a 5.5 MHz curvilinear transducer. Pancreas outlined by *arrows*. (**b**) Ultrasound of the thyroid using an 11 MHz linear transducer. Thyroid outlined by *arrows*

12.4 Ultrasound Transducer

12.4.1 Transducer

Ultrasound is generated by a transducer which contains one or more crystals composed of ceramic or naturally occuring piezoelectric materials. Such an example is quartz which following exposure to an applied voltage will provide a consistent mechanical vibration of 32.768 kHz. A quartz crystal commonly provides the fundamental timing element for watches. Examples of synthetic piezoelectric materials include ceramics such as lead-zirconate-titanate (PZT) or plastic composites such as polyvinylidene difluoride (PVDF).

The piezoelectric material converts an electrical pulse from the ultrasound machine's pulse generator into acoustic energy which can be transmitted for imaging. The electrical pulse induces a change in shape of the piezoelectric material. The expansion and contraction of the piezoelectric material propagates an acoustic wave with compression and rarefaction of a pressure amplitude front. Following interaction of the transmitted pulse with tissue, the transducer will function as a receiver and will detect the returning echoes. The returning acoustic energy deforms the piezoelectric material and generates a sequence of electric signals which are transferred to the ultrasound unit to help create a medical image. An ultrasound transducer can be used in both pulsed and continuous wave mode. In medical imaging, ultrasound is primarily used in pulse wave mode.

The natural resonance frequency of the crystal (f_o) is determined by the crystal's thickness. The wavelength of the emitted sound pulse is twice the thickness of the crystal. Using Eq. (12.1):

$$f_o = c*(2*t) \tag{12.11}$$

where c is the speed of sound in PZT (4000 m/sec) and t is the crystal thickness.

12.4.1.1 The Q Factor

When a crystal is excited, ultrasound energy is generated which is directed both in front of and behind the transducer. To improve the purity of the sound pulse, a damping block is positioned along the back of the piezoelectric element. The damping block will absorb the sound energy directed backward from the piezoelectric element and dampen the transducer vibration. This process of dampening the transducer vibration is called "ring down" and results in shortening of the spatial pulse length (SPL) of the emitted sound pulse. For medical imaging, ultrasound is predominantly used in pulse echo mode. With this approach, a burst of emitted ultrasound cycles are emitted for a finite period of time. The SPL is the summated distance of the transmitted ultrasound pulse. For an ultrasound pulse with three emitted wave cycles, the SPL is equal to 3 times the wavelength (λ). The frequency of how often this string of three successive wave cycle is emitted is referred to as the pulse repetition frequency. By shortening the SPL, the axial resolution of the transmitted pulse is improved (see section on spatial resolution).

Through the process of dampening the transducer's vibration, the bandwidth of the ultrasound pulse or range of transmitted frequencies is increased. Dampening introduces frequencies both above and below the center resonance frequency. The Q factor reflects the extent of the bandwidth or frequency range originating from the transducer.

$$\mathrm{Q} = \frac{fo}{\text{bandwidth}} \tag{12.12}$$

A high Q factor reflects a narrow bandwidth with little associated damping, while a low Q factor reflects a wider bandwidth with a greater degree of associated damping. Since many imaging applications demand increased axial resolution (the ability to distinguish adjacent objects along the axis of ultrasound beam transmission), low Q transducers are frequently used with their smaller SPL. For color Doppler imaging, transducers with a high Q are needed. The smaller bandwidth helps to preserve the frequency shift information which is critical to color Doppler imaging (Fig. 12.8).

12.4.1.2 Matching Layer

In order to minimize the acoustic impedance mismatch between the transducer surface and the patient, a layer of material is positioned in front of the transducer between the soft tissue and the piezoelectric material. This material or matching layer has an acoustic impedance or Z intermediate to that of the soft tissue and the piezoelectric crystal. The thickness of the matching layer is chosen so that it is ¼ of the wavelength of the transmitted pulse as determined by the f_o.

In addition to using a matching layer, the acoustic mismatch between the transducer surface and the patient is also reduced by using ultrasound gel or jelly.

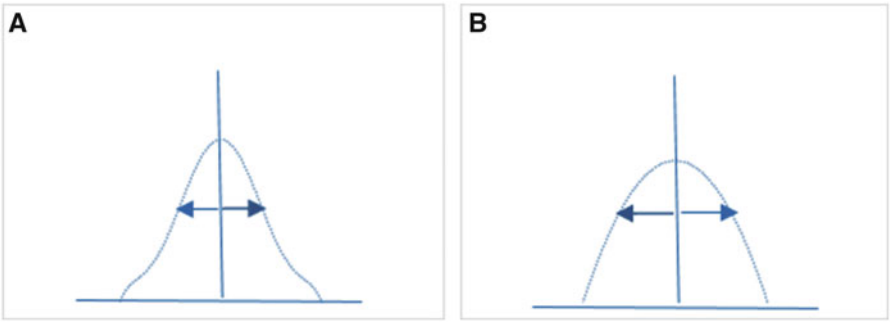

Fig. 12.8 *Q factor*. The figures below demonstrate frequency spectrum for transducers with a narrow (**a**) and a wide bandwidth (**b**). The Q factor is equal to the center frequency (f_o) divided by the bandwidth. A high Q transducer (**a**) has very little damping, while a low Q transducer (**b**) has heavier damping

The ultrasound gel also has the added benefit of helping remove air pockets between the transducer surface and the patient's skin.

12.4.2 Types of Transducers

Modern-day medical transducers consist of either linear or curvilinear arrays composed of many rectangular piezoelectric elements. Within the transducer, there may be anywhere from 128 to 512 piezoelectric elements. Based upon the activation mode of how the ultrasound pulse is generated, transducers can be divided into two different types: (1) linear array and (2) phased array.

12.4.2.1 Linear Array

Within a linear array transducer, there is simultaneous activation of a small group of piezoelectric elements. For example, if the linear array transducer consists of 512 elements, the first activated group may consist of 32 activated piezoelectric elements. While the 32 element group is transmitting, the remaining transducer elements are then utilized for echo reception. Following the transmission of the first ultrasound pulse, a second small group of piezoelectric elements, usually removed from the first group by one or two piezoelectric elements, are activated and generate a second pulse. This sequential pattern of activation then continues across the remaining transducer surface. Through the sequential transmission and reception of pulse echoes, information for generating an ultrasound image is collected.

12.4.2.2 Phased Array

In contrast to a linear array, a phased array transducer produces a single ultrasound pulse from all of the transducer piezoelectric elements. With a phased array, a time delay is introduced in the process of activating the piezoelectric elements across the face of the transducer. Through the introduction of this time delay, the ultrasound pulse can be steered without moving the transducer at all. When the phased array listens for the returning echoes, all of the transducer elements are recruited, and the aggregate information from all of these elements is used to generate an image.

12.5 Ultrasound Beam Properties

For a single piezoelectric element, the transmitted ultrasound beam focuses upon a single point or focal point. The focal point occurs at a focal distance from the transducer surface and signifies where the sound energy converges. The distance preceding this point is referred to as the near field or Fresnel zone. The distance beyond this point is referred to as the far field or Fraunhofer zone. The majority of medical ultrasound imaging occurs within the near field. Within the far field, the ultrasound beam diverges and the intensity of the sound quickly attenuates.

12.5.1 The Near Field

The ultrasound energy within the near field converges toward the focal point. This property of beam convergence is the result of the constructive and destructive interactions between adjacent sound waves that occur just after the sound has been emitted from the transducer surface. The aggregate ultrasound beam converges at the focal distance which signifies the end of the near field (Fig. 12.9). At this point, the beam diameter is approximately half of the diameter of the transducer. The near-field length or focal distance depends upon the transducer diameter (d) and the wavelength of sound (λ) within the transmission medium:

$$\text{Focal Distance} = \frac{d^2}{4^*\lambda} \tag{12.13}$$

With an increase in the transducer diameter and/or an increase in the transmission frequency, the near-field distance will increase. As an example, with a 7.5 mm piezoelectric element, the near field at a transmission of 5 MHz is 4.6 cm, while the near field at a transmission of 7.5 MHz is 6.8 cm.

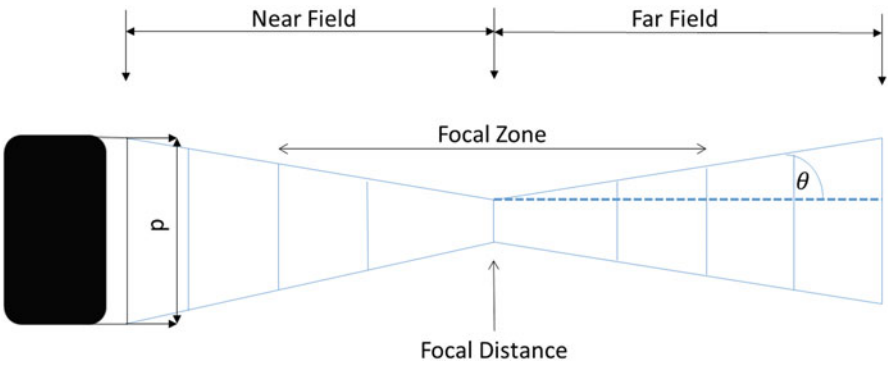

Fig. 12.9 *Near field and far field*. For a single element transducer, the ultrasound beam demonstrates a unique pattern with both a region of convergence, the near field, and a region of divergence, the far field. The length of the far field and the angle of divergence of the far field (Θ) vary with changes in the width of the piezoelectric element (d) and the λ of the transmitted pulse

12.5.2 The Far Field

The far field or Fraunhofer zone occurs beyond the outer limits of the near field and outlines where the ultrasound beam begins to diverge or widen (Fig. 12.9). The far field highlights where the ultrasound beam begins to rapidly attenuate or weaken in strength or signal intensity. The rate at which the beam diverges is determined by the angle of ultrasound beam divergence (Θ_{div}) where:

$$\text{Sin}\,(\Theta_{div}) = 1.22^{*}\frac{\lambda}{d} \tag{12.14}$$

The rate of beam divergence increases with a decrease in frequency and/or a decrease in the diameter of the emitting transducer. For example, with a 7.5 mm piezoelectric element and a transmission frequency of 5 MHz (or λ equal to 0.308 mm), the angle of ultrasound beam divergence equals 2.87°, while with a frequency of transmission of 7.5 MHz, the angle of ultrasound beam divergence equals 1.91°.

12.5.3 Ultrasound Beam Formation and Focusing

Optimal medical imaging occurs within the focal zone (Fig. 12.9). The focal zone comprises the distal end of the near field and the proximal end of the far field. The focal zone is defined as the distance over which the width of the transmitted ultrasound beam is no greater than two times the width of the ultrasound beam at the focal distance. Since the best medical images will occur within the focal zone, this fact impacts the type of transducer that the technologist will choose.

Clinically, the most frequently used transducers are linear array or phased array transducers rather than single element transducers. The above discussion of ultrasound beam properties focused upon a single element transducer. How do these properties change with multi-array transducers?

For a linear array transducer, groups of piezoelectric elements are sequentially activated across the face of the transducer. When determining the near field, the transducer diameter is equivalent to the width of the simultaneously activated group of piezoelectric elements.

For a phased array transducer, the piezoelectric elements are near simultaneously activated across the face of the transducer but with the introduction of a small time delay from one piezoelectric element to the next. By varying this small time delay and the location of the initial piezoelectric element activation, the ultrasound beam can be modified to converge at selectable focal distances. In abdominal imaging, you may be interested in focusing the transducer upon a more shallow structure. For example, the patient may have a mass in the liver along the outer surface. In such a situation, you are interested in a smaller focal distance (Fig. 12.10). In the same patient after you have finished imaging the liver, the technologist will then want to evaluate structures deeper within the abdomen such as the inferior vena cava or pancreas, and a larger focal distance will be needed (Fig. 12.10). When first imaging the outer surface of the liver, a shorter focal distance will be chosen by first activating the piezoelectric elements at the periphery of the transducer followed by sequential activation of the remaining piezoelectric elements as we progress toward the center of the probe. When imaging the pancreas, the focal distance can be increased by decreasing the delay time between sequential activation of individual piezoelectric elements. By reducing the delay time, this change causes the aggregate ultrasound beam to converge at a greater depth.

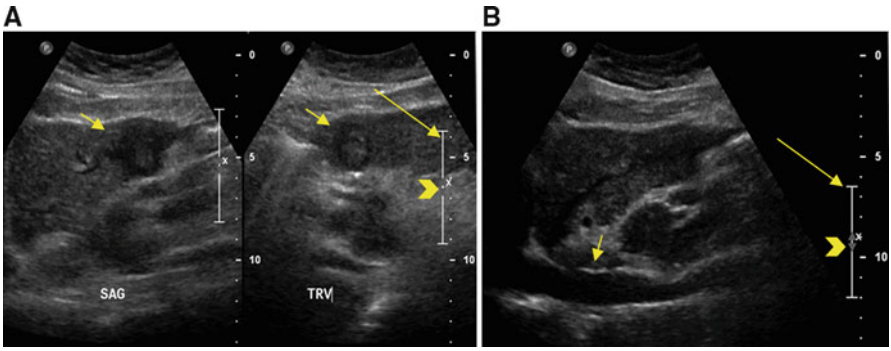

Fig. 12.10 *Different focal distances using a phased array transducer to image the abdomen.* For a phased array transducer, these two images demonstrate the ability to vary the depth of the focal zone and focal distance. (**a**) This is an image of a mass (*small arrow*) within the periphery of the left lateral segment of the liver. The *large arrow* highlights the focal zone, while the chevron illustrates the focal distance. (**b**) This is an image of the inferior vena cava (*small arrow*), the large vein located deep within the abdomen, just above the spine. Notice the positioning of the focal zone (*large arrow*) and focal distance (*chevron*) at a greater depth of penetration

When creating the displayed medical image, all of the piezoelectric elements within the array transducer will receive information from returning echoes. This information will be summed together to generate the image displayed on the monitor. The echo signal received by the piezoelectric elements along the periphery of the transducer will have traveled a greater distance than the elements in the center of the transducer. Just as the ultrasound beam converges toward the focal distance, the returning echoes must diverge out to the periphery of the transducer (Fig. 12.9). Since the received echoes from the outer piezoelectric elements will have traveled a greater distance, their signal will be delayed in time with respect to the reception of the received signals from the elements toward the center of the transducer. To align the timing of the signals, electronic delays are introduced to the earlier received signal before their information is added to the signals from the later received echoes. This process is called dynamic receive focusing.

12.5.4 Ultrasound Spatial Resolution

The spatial resolution of ultrasound imaging is described in three different dimensions: axial, lateral, and elevational. Each of these dimensions helps to detail the volume of the acoustic pulse. The smaller the volume of the emitted acoustic pulse augments the ability of the ultrasound pulse to distinguish between two adjacent objects (Fig. 12.1b and discussion of imaging resolution).

12.5.4.1 Axial Resolution

Axial resolution reflects how well ultrasound imaging can distinguish between two objects which are next to each other and are in line with the direction of the emitted ultrasound beam. In order to achieve good axial resolution, the returning echoes cannot overlap and must maintain distinction from the trailing echo. In order to avoid overlap, two imaged objects must be separated from each other by a distance greater than or equal to one-half of the spatial pulse length (SPL). As discussed earlier, the SPL is the summated distance of the transmitted ultrasound pulse. If objects are closer than ½ SPL, the returning echoes will overlap, and the adjacent objects cannot be resolved.

For example, if a 3.5 MHz transducer is being used, the wavelength of the pulse is equal to 0.51 mm. For an ultrasound pulse with 3 cycles, the SPL is equal to 1.53 mm. In order to distinguish two adjacent objects along the direction of the ultrasound beam, they have to be separated by greater than ½ SPL or 0.765 mm. For this example, the axial resolution is equal to 0.765 mm (Fig. 12.11). If the distance separating the two objects is less than 0.765 mm, overlap or volume averaging of the two objects will occur. This concept of volume averaging is further discussed in the slice thickness artifact section (Fig. 12.23).

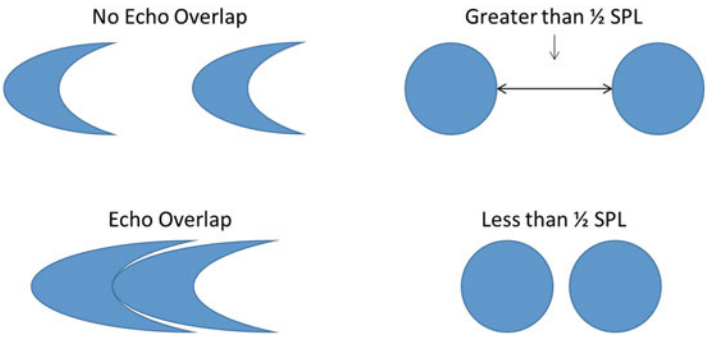

Fig. 12.11 *Axial resolution*. In order to distinguish two adjacent objects along the axial plane of the ultrasound pulse, the distance separating the two objects must exceed ½ of the spatial pulse length (SPL). If the distance does not exceed ½ of the SPL, the returning echoes will overlap, and the two objects will be volume averaged into one structure on the displayed image

12.5.4.2 Lateral Resolution

Lateral resolution reflects the ability of ultrasound to distinguish between two adjacent objects which are at a 90° angle to the direction of the ultrasound beam. The lateral resolution is reflected by the diameter of the ultrasound beam. As the diameter of the ultrasound beam decreases, the lateral resolution improves. As discussed earlier, the beam diameter will vary with distance from the transducer. The best lateral resolution is achieved within the focal zone. The ideal point of imaging occurs at the focal distance where the ultrasound beam is the narrowest. Beyond the outer limit of the focal zone, the beam will continue to diverge, and the lateral resolution will quickly deteriorate (Fig. 12.12). The typical lateral resolution is between 2 and 5 mm.

Phased array transducers help to optimize lateral resolution. Phased array transducers can vary the focal distance of the transmitted ultrasound pulse by altering the timing delay of piezoelectric element activation. By being able to change the focal distance and emit several different ultrasound pulses, the lateral resolution can be preserved even with increasing distance from the transducer. This objective is accomplished by transmitting successive pulse echoes with an overlap of focal zones with increasing depth into the tissue. This approach effectively increases the length of the focal zone and avoids the rapid decay of the lateral resolution. Since this method requires multiple pulse echo sequences to be transmitted along a single beam line, the frame rate or amount of time needed to create an image increases.

12.5.4.3 Elevational Resolution

Elevational resolution reflects the ability of the ultrasound beam to distinguish two adjacent objects which are perpendicular to the imaging plane (Fig. 12.12). Elevational resolution varies based upon the height of the transducer element. As the height of the transducer element decreases, the elevational resolution improves.

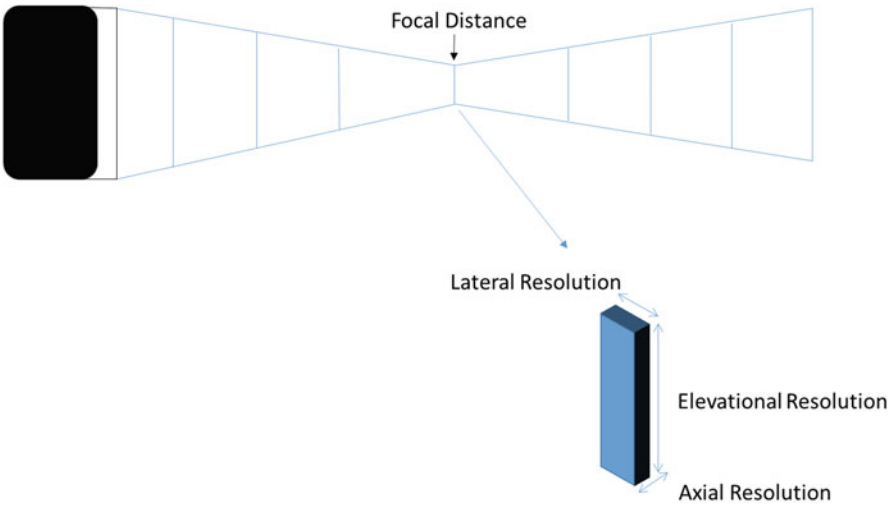

Fig. 12.12 *Lateral resolution and imaging volume*. The lateral resolution reflects the ability to distinguish two adjacent objects which are within the imaging plane but at a 90° angle to the direction of the propagating ultrasound pulse. Lateral resolution improves as the width of the ultrasound beam decreases. The optimal lateral resolution occurs at the focal distance where the beam width is the narrowest. At the focal distance, an imaging volume is detailed. The three dimensions of spatial resolution (*axial*, *lateral*, *and elevational*) are illustrated

Elevational resolution is also referred to as the slice thickness. As the slice thickness increases, objects that are contained within that imaging volume are averaged across the imaging plane. Since the object's echo is averaged over a larger volume, the object's outline will lose some of its distinction or resolvability. This concept of volume averaging is further discussed in the slice thickness artifact section (Fig. 12.23).

12.6 Ultrasound Image Acquisition

Ultrasound images are acquired by emitting a train of short pulses with a duration of less than 1 μs. In between pulses, the transducer listens for the echoes. This method is called pulse echo. The longer the amount of time that it takes an echo to return to the transducer, then the more attenuated the signal amplitude becomes. The extent of attenuation provides information regarding the depth of the imaged object. To improve image quality and uniformity, the signal of the returning echo can be amplified using time gain compensation (TGC). TGC is a dynamic adjustment that will vary the signal gain for echoes that take longer to return to the transducer. This process will compensate for the attenuation that occurs with greater depth.

For example, a greater degree of TGC will be applied to echoes returning from the inferior vena cava than echoes returning from the capsular surface of the liver (Kremkau 1993).

12.6.1 Types of Echo Display

The returning echo to the transducer can be displayed in one of three different ways: A-mode, B-mode, and M-mode.

12.6.1.1 A-Mode

A-mode represented the first type of ultrasound display and stands for amplitude mode. Echo amplitude was displayed on the vertical axis, while echo return time was displayed on the horizontal axis. As described earlier, echo return time is an indication of depth or distance of a tissue interface from the transducer. One A-line of data was generated for each pulse repetition period. Initially, A-mode was used to evaluate midline displacement of the brain in patients suffering from a brain tumor. Today, A-mode can be used by ophthalmologists (eye doctors) for precise measurements of the eye.

12.6.1.2 B-Mode

B-mode displays a grayscale image of a tissue section and stands for brightness mode. The greater the intensity of the returning echo, then the greater the displayed signal brightness or level of echogenicity. The returned echoes are displayed as a function of depth from the transducer and position across the sector scan of the emitted ultrasound beam. Essentially, one 2D B-mode image is generated by a number of A-lines spanning across the transducer's field of view. Using a multielement phased array transducer, real-time imaging can be performed with 15–40 frames (grayscale static images) being displayed per second. The frame rate or number of static images displayed per second inversely relates to the number of A-lines used to compose the frame (N) and the depth of tissue (D) from where the echoes are returning. When the amount of data (N) used to compose the static image increases or the depth of ultrasound penetration (D) lengthens, the frame rate will decrease. For example, if the density of scan lines (scan lines per centimeter) is increased in order to provide enhanced axial resolution, the frame rate will decrease. Also, if a deeper anatomical structure such as the inferior vena cava (the large vein that lies next to the spine) is imaged, the frame rate will also drop.

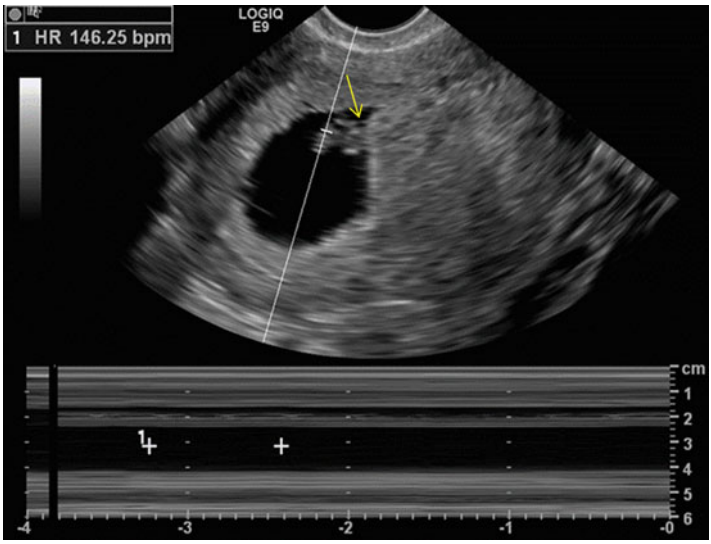

Fig. 12.13 *M-mode image*: This is an M-mode image focused on a single tissue interface of the beating heart of a fetus with an estimated gestational age of 6 weeks. Note the M-mode display on the bottom of the grayscale image. Also note how the point of interrogation is fixed on one point (*arrow*)

12.6.1.3 M-Mode

This technique stands for motion mode. This imaging approach uses the signal from B-mode imaging to describe the echoes of a moving structure such as the heart with the transducer oriented on a fixed position or tissue interface within the patient. M-mode displays depth on the vertical axis and time on the horizontal axis. By displaying successive ultrasound pulses next to each other, the change in the position of a single tissue interface can be monitored, and M-mode can be used to illustrate time-dependent motion. This display technique can be used to focus on the tissue interface of a beating heart and to help estimate the heart rate of a 6-week live fetus (Fig. 12.13). M-mode can only focus on the motion of a single tissue interface or line through the patient. Given this limitation and advancements in two-dimensional echocardiography, this technique has been largely replaced by color Doppler imaging.

12.6.2 Components of an Ultrasound Machine

For the pulse echo method of ultrasound image acquisition, several hardware components are needed within the ultrasound machine including: a beam former, a pulser, a receiver, a scan converter, and a video display.

12.6.2.1 Beam Former

The beam former performs the previously discussed process of dynamic receive focusing (see section on *ultrasound beam formation and focusing*). The beam former applies electronic delays to help align the phases of the echoes returning to the many individual elements of an array transducer. The realigned signals from all the transducer elements are then summated, creating an output signal which represents the acoustic information from a pulsed ultrasound beam.

12.6.2.2 Pulser

The pulser generates the electric voltage which is applied to the piezoelectric elements within the transducer and produces the acoustic signal.

12.6.2.3 Receiver

The receiver accepts signal information from the beam former and performs post-processing such as TGC and filtering of noise and clutter.

12.6.2.4 Scan Converter

Scan converter is a device within the ultrasound machine that takes the signal information from the returning echo and translates it into a data format which can be displayed as a 2D image. The data format from scan acquisition and scan display are very different, and the scan converter is a critical hardware piece for a functional ultrasound machine to display a medical image that can be read by a clinician. Initially, scan converters were analog devices that used storage cathode ray tubes to consolidate image data. Modern-day scan converters use digital methods for data processing and storage.

Image data is stored into a 512×512 matrix of pixel elements where each pixel corresponds to a rectangular coordinate on the image display. During image acquisition, the returning echo is processed by the scan converter, generating a digital signal. This digital information is assigned to a pixel within the image data matrix based upon the orientation of the transducer beam and the time needed for the echo to return to the transducer (echo delay time). For a grayscale ultrasound image, one displayed image frame requires 0.25 MB of memory storage. The amount of memory storage is equivalent to the image data matrix size (512×512) times the number of bytes per grayscale pixel which is equal to one. One byte is equivalent to 8 bits where each pixel can display up to 256 or 2^8 different grayscale levels. For color Doppler images, 3 bytes of storage are needed per color scale pixel.

12.6.2.5 Video Display

Once the digital information is acquired and assigned to a memory location, the digital to analog converter converts the matrix of digital data into an analog signal which can be displayed on a video monitor. In addition to the grayscale information from a 2D B-mode image, the video display can show information acquired from M-mode and Doppler ultrasound.

12.7 Doppler Ultrasound

Up to this point, discussion has focused upon the generation of grayscale ultrasound imaging. These grayscale images are composed from pressure amplitude information regarding returning echoes which have either been reflected or scattered. Additional imaging information can also be found in the frequency variation of the returning echoes. This detection of a change in echo frequency serves as the basis for Doppler ultrasound imaging.

Frequency shift occurs when incident sound energy reflects off a moving object. If the object is moving away from the source of sound, the returning echo travels at a lower frequency than the initial incident sound, while if the object is moving toward the source of sound, the returning echoes travel at a higher frequency than the initial incident sound. The Doppler frequency shift (F_d) is defined as the difference in frequency between the initial incident sound (F_t) and the returning echo (F_r).

$$F_d = F_t - F_r \tag{12.15}$$

A practical application of this effect is noticed when an ambulance travels by you. As the ambulance approaches a stationary listener, the emitted siren noise demonstrates an even higher frequency (or higher audible pitch) as the emitted sound undergoes a Doppler frequency shift from the forward motion of the ambulance. Similarly, as the ambulance moves away from the stationary listener, the audible sound heard by the listener exhibits a lower frequency (or attenuated audible pitch) from the sound emitted by the siren. The frequency shift (F_d) is defined by the following equation:

$$F_d = 2 * F_t * \left(\frac{V}{c}\right) * \cos(\theta) \tag{12.16}$$

c is the speed of the transmitted sound, and V is the speed of the moving object. θ is the angle between the transmitted sound and the direction of blood flow or moving red blood cells (Fig. 12.14). On an ultrasound image, θ is measured by adding the angle indicator line (Fig. 12.15). If the transducer is perpendicular to blood flow, no frequency shift can be detected since the cos (90°) is equal to zero. Optimal imaging

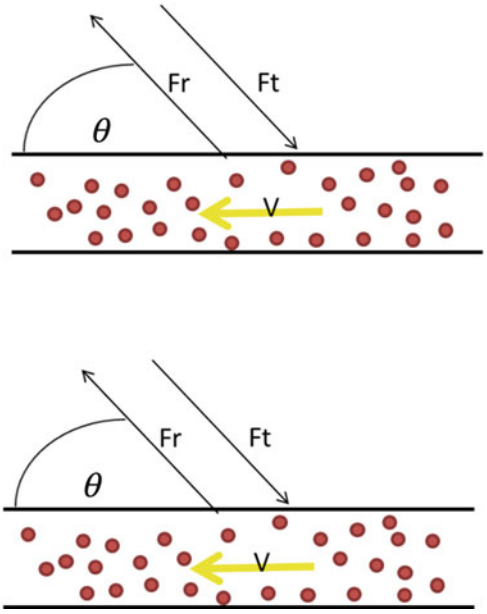

Fig. 12.14 *Doppler ultrasound: Doppler frequency shift.* Incident sound energy is transmitted as F_t. This energy is then reflected and scattered off of moving red blood cells with echoes (F_r) returning to the ultrasound transducer. Θ is the angle between the incident sound energy and the direction of the flowing red blood cells. V is the velocity of a red blood cell

is performed with the transducer as close as parallel to the vessel of interest so that the cos (θ) is maximized. As demonstrated by Eq. (12.16), velocity (V) is directly proportional to frequency shift. For Doppler ultrasound imaging, the moving object is usually a red blood cell in either a vein or artery. When the sound hits the moving red blood cell, the incident energy is both reflected and scattered. When the transducer detects the returning echo, the change in frequency can be used to measure the velocity of the blood. In addition, detailed color maps can be generated which outline the anatomy of the vasculature tree and potentially highlight such disease processes as atherosclerotic disease or plaque formation along the vessel wall.

We have introduced two different concepts in this discussion, blood flow and blood velocity. Blood velocity measures the rate that a particle of interest, i.e., a red blood cell, travels per unit time. Blood velocity is measured in cm/sec. Blood flow measures the volume of blood that travels per unit time and is measured in cm^3/sec.

Under conditions of fully developed, steady-state flow, the blood flow is related to the mean velocity by the following equation:

$$\text{Flow} = V * A \tag{12.17}$$

where V is the mean velocity and A is the cross-sectional area of the vessel.

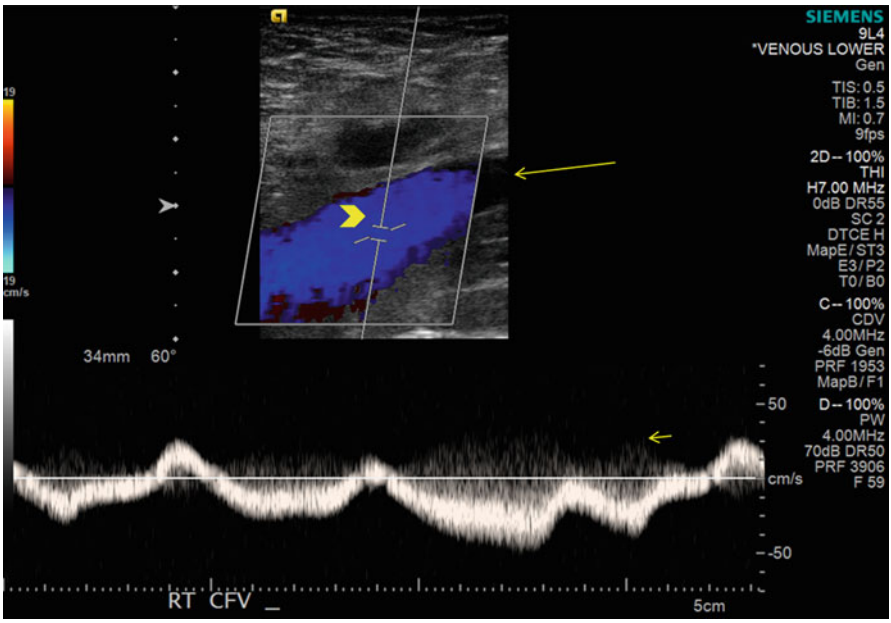

Fig. 12.15 *Duplex Doppler ultrasound:* The center box (*large arrow*) displays the grayscale image. The trapezoid represents the Doppler sample volume. The angle indicator line (*chevron*) provides a quantitative measurement of Θ or the Doppler angle. The velocity of the blood as a function of time is displayed by the graph on the bottom of the image (*small arrow*). The *blue color* within the vessel and the velocity below the zero line highlights flow away from the transducer

Pulsed Doppler imaging can evaluate both velocity and range (or the distance from where the moving object originates). The transducer obtains information from a specific location of interest or the Doppler sample volume. The size of the Doppler sample volume can be changed by adjusting the amount of time that the transducer receives or listens for returning echoes. By first imaging with grayscale ultrasound imaging, the vessels of interest can be visualized, and the Doppler sample volume can be positioned within the lumen of the vessel which will be evaluated. Duplex scanning is defined as this combined use of both grayscale and pulsed Doppler imaging (Fig. 12.15). The velocity is represented on the vertical scale, while time is indicated on the horizontal scale. When flow is toward the transducer, this results in a positive frequency shift and a positive magnitude velocity value, while the opposite relation holds true for flow away from the transducer. Generally, flow toward the ultrasound transducer is color-coded as red, while flow away from the transducer is color-coded as blue (Fig. 12.15).

Aliasing represents the most significant artifact associated with Doppler ultrasound imaging. According to the Nyquist criteria, the sampling rate must exceed twice the highest frequency component of the sampled signal. Practically, this means that the rate at which the ultrasound transducer evaluates the Doppler frequency shift must exceed twice the magnitude of the frequency shift. If the

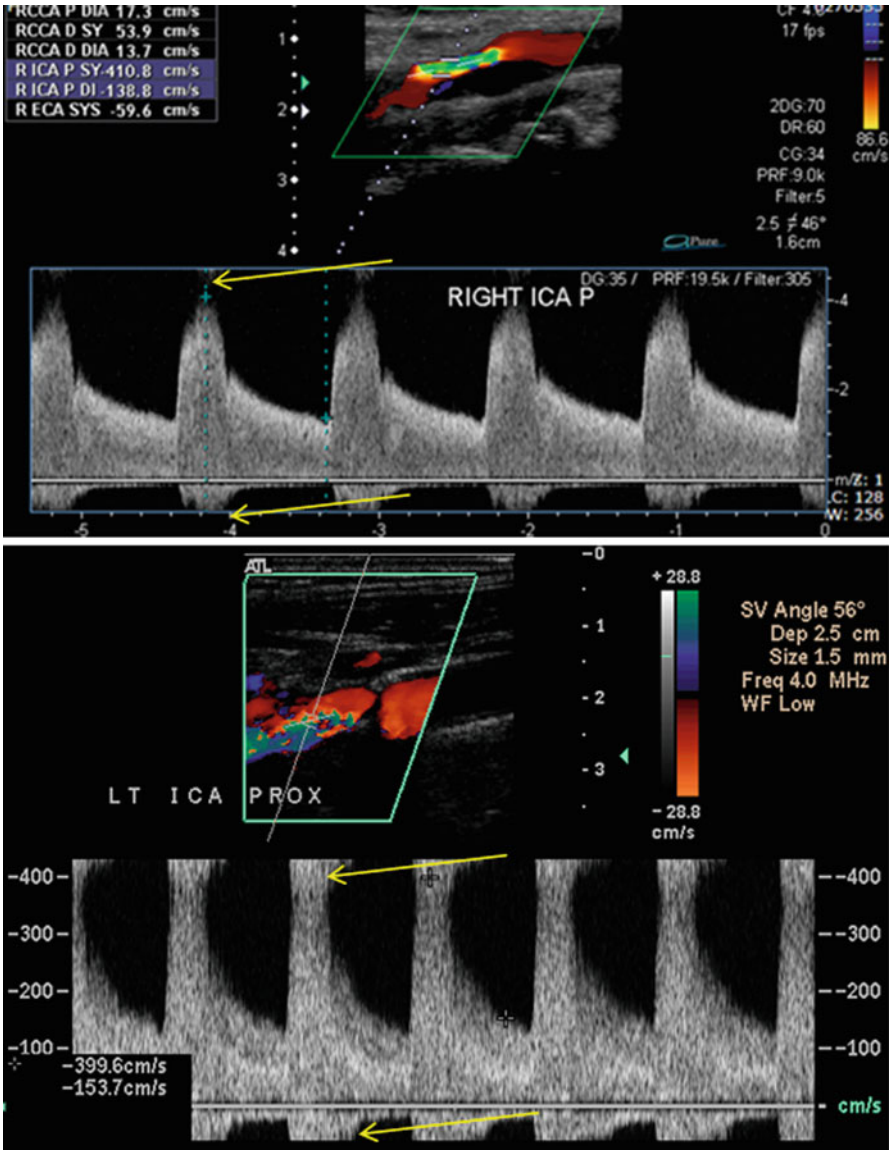

Fig. 12.16 *Aliasing*. When the Nyquist criteria are not satisfied, undersampling occurs which results in aliasing. With aliasing, the high-frequency components are wrapped around from the negative end of the scale to the positive end of the scale (*long arrows*)

Nyquist criteria are not satisfied, undersampling occurs which results in the artifact of aliasing. When aliasing occurs, the high-frequency components are wrapped around from the positive end of the scale to the negative end of the scale (Fig. 12.16). Aliasing can be addressed in several ways. The most easily executed method is to increase the sampling rate or the pulse repetition frequency (PRF).

The PRF reflects how many packets of successive sound cycles are emitted per second (also discussed in the Q factor section). For example, in pulse echo mode, three successive cycles of sound (or a packet) are sent out at 3000 times per second for a PRF of 3KHz. The PRF is not to be confused with the inherent frequency of 1 cycle of generated sound which composes one of the 3 cycles of the packet or sonic pulse. For example, in abdominal imaging, the inherent frequency of 1 cycle is generated by a 3.5 MHz phased array transducer. Generally speaking, the PRF will be measured in kHz, while the frequency of the sound wave is measured in MHz.

Returning to the subject of aliasing, increasing the PRF can eliminate this artifact. If the frequency shift (F_d) is 1.5 kHz, then the PRF must satisfy the Nyquist criteria and be greater than 3 kHz or greater than two times the frequency shift. Practically, an increase in the PRF increases the scale of the Doppler display and allows for a display of higher velocity values. Other methods of decreasing aliasing involve decreasing the extent of the frequency shift such as by making the value of cos (θ) smaller by increasing the Doppler angle. Lastly, aliasing can be reduced by using a lower-frequency probe or decreasing the frequency of the sound waves which compose the sound packet or sonic pulse (Bude and Rubin 1996; Rubin 1994).

12.7.1 Color Doppler

Color Doppler provides an excellent means to evaluate vessel anatomy, vessel patency, flow direction within the vessels, and magnitude of velocity. Color Doppler displays real-time color Doppler data which is superimposed upon a grayscale ultrasound image. The grayscale image provides information regarding the vessel morphology. Velocity is represented by color data where a higher velocity (greater frequency shift) is indicated by a lighter color, while a lower velocity (smaller frequency shift) is displayed with a darker color. The direction of the flow is reflected by red hues which signify flow toward the transducer and blue hues which indicate flow away from the transducer. Color Doppler provides useful information regarding small structures that may be difficult to evaluate with pulsed Doppler. For example, small vessels such as the pampiniform plexus in the scrotum can be evaluated for vessel patency. Additionally, color Doppler is very useful for demonstrating the vascularity of a mass such as a thyroid nodule (Fig. 12.17).

12.7.2 Power Doppler

Power Doppler displays patency or flow within a vessel but without quantitative information related to velocity or flow direction. Power Doppler detects the frequency shift but does not preserve the information that allows for a measurement of

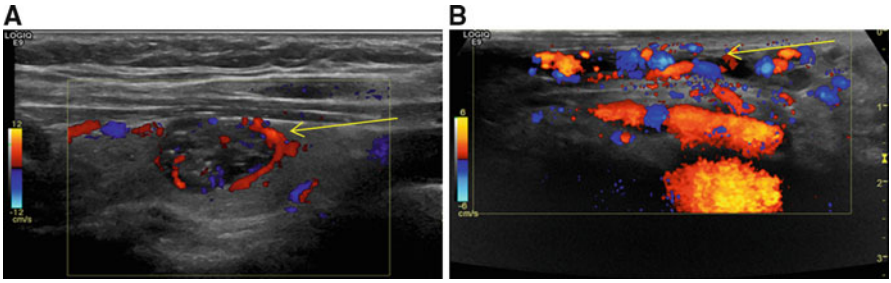

Fig. 12.17 *Doppler imaging*. (**a**) Color Doppler imaging demonstrates flow (*arrow*) within a solid thyroid nodule. (**b**) Color Doppler imaging demonstrates flow (*arrow*) within the pampiniform plexus of the male spermatic cord

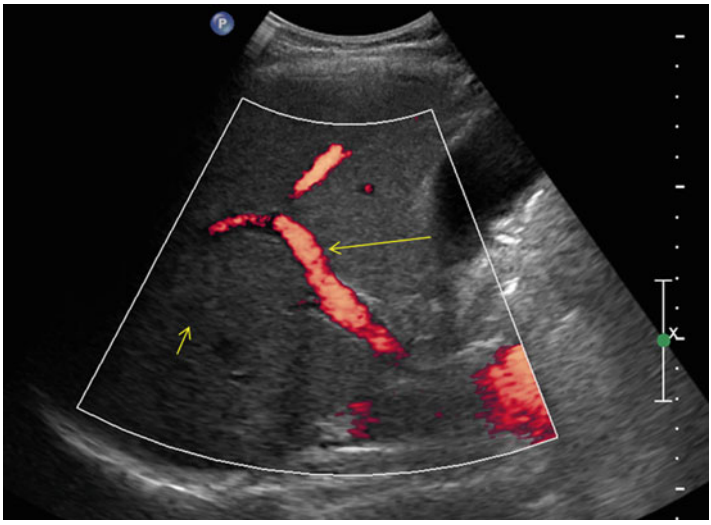

Fig. 12.18 *Power Doppler*. The power Doppler image displays patent flow within the portal vein (*long arrow*) of the liver (*short arrow*). No quantitative information is provided in regard to the direction of flow or the magnitude of the velocity

velocity magnitude or phase. Instead, power Doppler imaging measures only the strength of the returned Doppler signal. Since power Doppler does not preserve the frequency information, the Doppler angle is not as critical a component as with pulsed Doppler, and flow traveling near perpendicular to the transmitted sound can be detected. Power Doppler has the advantage of being slightly more sensitive to blood flow detection. This feature allows for its application in detecting slow blood flow within small vessels. Since power Doppler discards the frequency shift information, aliasing artifacts do not occur. Practically, power Doppler is only utilized when color Doppler fails to demonstrate flow patency. Since velocity and phase information is lost, power Doppler can only highlight whether flow is present or absent (Fig. 12.18).

12.7.3 Ultrasound Artifacts

With all of medical imaging, misrepresentations of imaged structures or artifacts provide an inaccurate description of the imaged area. While artifacts can impair the image quality, sometimes they are used to help characterize the tissue of interest and provide additional information about its internal composition. Some of these artifacts have been described previously, and this section will help complete the discussion.

12.7.3.1 Mirror Images

Mirror images occur where there is near-complete reflection of the incident ultrasound signal. This occurs frequently at an air-soft tissue interface such as the base of the lungs. In the right upper quadrant, the air-soft tissue interface with the right hemidiaphragm can produce mirror images of the liver and/or masses within the liver (Fig. 12.19).

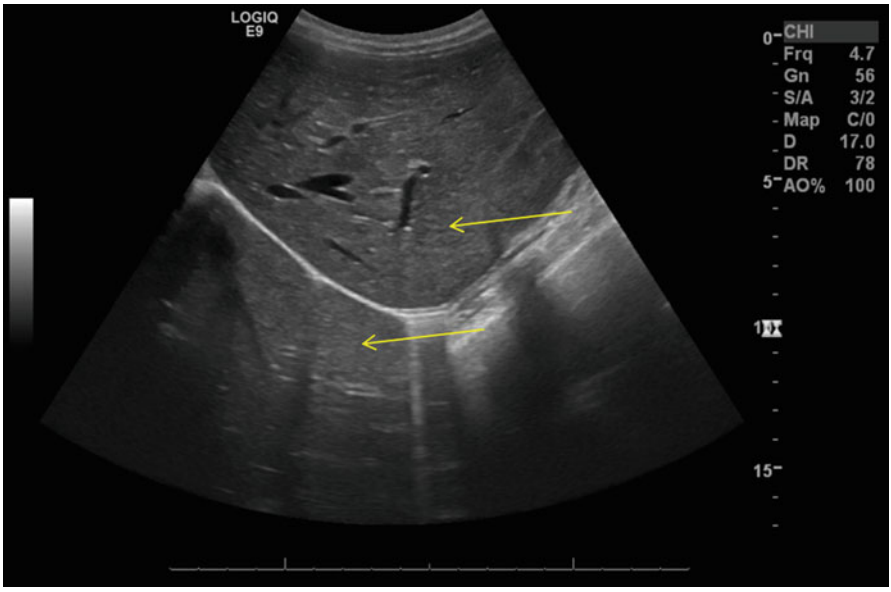

Fig. 12.19 *Mirror image artifact*. This artifact occurs at a tissue interface where complete reflection occurs. An example would be an air-soft tissue interface such as the hemidiaphragm which separates the lungs (air containing) from the abdomen (soft tissue containing). At this interface, a mirror image of the liver (two *long arrows*) is created

12.7.3.2 Reverberation

Reverberation occurs from multiple reflections of the same ultrasound pulse at an acoustic interface. This interaction occurs when the ultrasound beam is reflected at an acoustic interface which is positioned within the near field of the ultrasound beam. The returning echo is then reflected off the transducer, resulting in a second interaction and potentially additional cascading interactions with the same interface. This process can generate multiple reflections or reverberations. How does the reverberation artifact affect the displayed image? The reverberation can give the appearance that the acoustic interface is more deeply positioned within the tissue. This artifact is best seen when imaging a fluid contained structure such as the bladder. The reverberation can lead to low-level internal echoes within the bladder that should otherwise appear black or anechoic (Fig. 12.20). The low-level echoes within the bladder result from the reverberations generated by the overlying soft tissue superficial to the bladder being displaced into the anechoic center of the bladder. Generally, the reverberation artifacts are not visible for they are superimposed onto a background signal of soft tissue; and therefore, they cannot be seen.

Ring down or comet tail artifacts are also a type of reverberation artifact. These artifacts occur when the incident ultrasound pulse interacts either with gas, cholesterol crystals, or metal. The incident ultrasound energy bounces off the highly reflective interface of the metal, crystal, or gas only to be immediately reflected again by another highly reflective interface caused by an adjacent focus of gas,

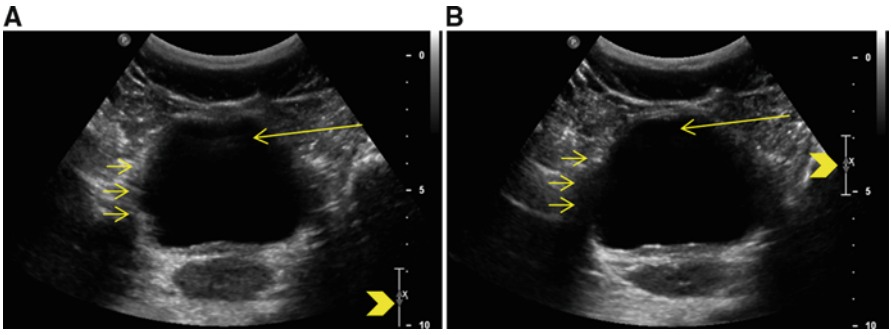

Fig. 12.20 *Reverberation artifact*. In image (**a**), there are low-level echoes (*long arrow*) within the superior aspect of the bladder (outlined by *short arrows*). These echoes are evident when the bladder is imaged well within the near field. Note the position of the focal zone in the lower left corner of the image (*chevron*). How do these reverberation artifacts arise? The incident sound initially reflects off the soft tissue/bladder interface. This echo can then reflect off the transducer probe only to be reflected again by the same soft tissue/bladder interface, creating a cascade of echoes (reverberation artifacts) which appear to originate deep to the original bladder/soft tissue interface. Normally, these echoes are lost within the background of the soft tissue, but they become more conspicuous when imaging an anechoic structure such as the bladder within the near field. In image (**b**), the focal zone is repositioned so that the bladder is positioned within the center of the focal zone, and the reverberation artifacts disappear

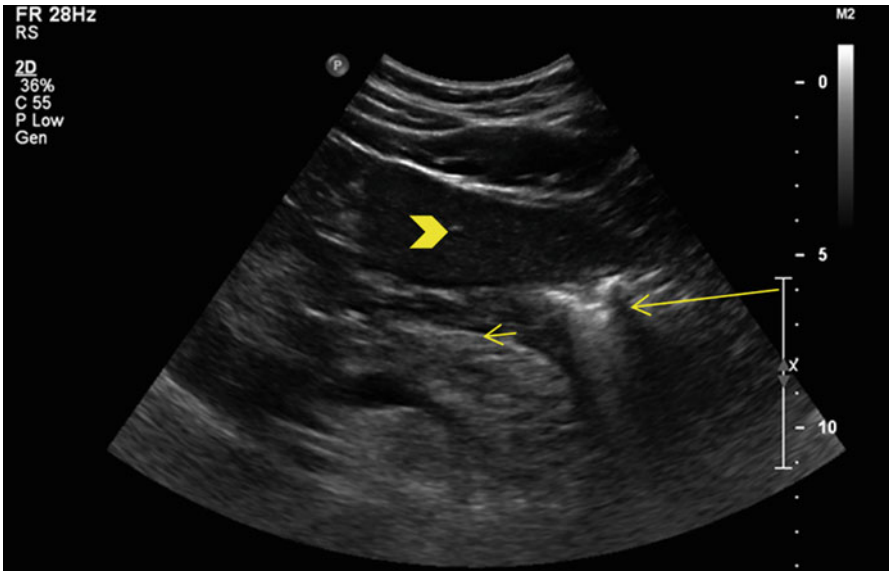

Fig. 12.21 *Ring down artifact*. Ring down artifact (*long arrow*) originating from a gas filled loop of small bowel is demonstrated along the undersurface of the liver (*chevron*). The pancreas is also visible within this image (*small arrow*)

crystal, or metal. Since these reflective interactions occur within such a small area, the returning echo is perceived by the transducer as representing a singular echo. With each reflective interaction, the echo amplitude decreases, and the echo will resemble a "comet tail" with weakening signal strength as distance from the ultrasound transducer increases. Overall, these interactions will give the appearance of multiple bright echoes originating deep to the original site of reflection with the gas, metal, or crystal (Fig. 12.21).

12.7.3.3 Side Lobes and Grating Lobes

When the piezoelectric element is exposed to a voltage, a sound beam is generated in the general direction of crystal distortion. A small amount of crystal distortion occurs orthogonal or radial to this central axis and generates weak side lobes of ultrasound energy which radiate off-axis from the central sound beam. If these weak side lobes interact with a reflector, they can produce an echo artifact. When imaging soft tissue, these side lobes are frequently concealed by the background scatter signal, but when imaging an anechoic fluid-filled structure such as a cyst or the gallbladder, they can become more conspicuous (Fig. 12.22). This side lobe artifact can simulate the appearance of sludge (or pseudosludge) within a homogeneously echo-free organ.

Grating lobe artifacts arise from multielement array transducers and are emitted at large angles to the transducer surface. This artifact is created by the composition

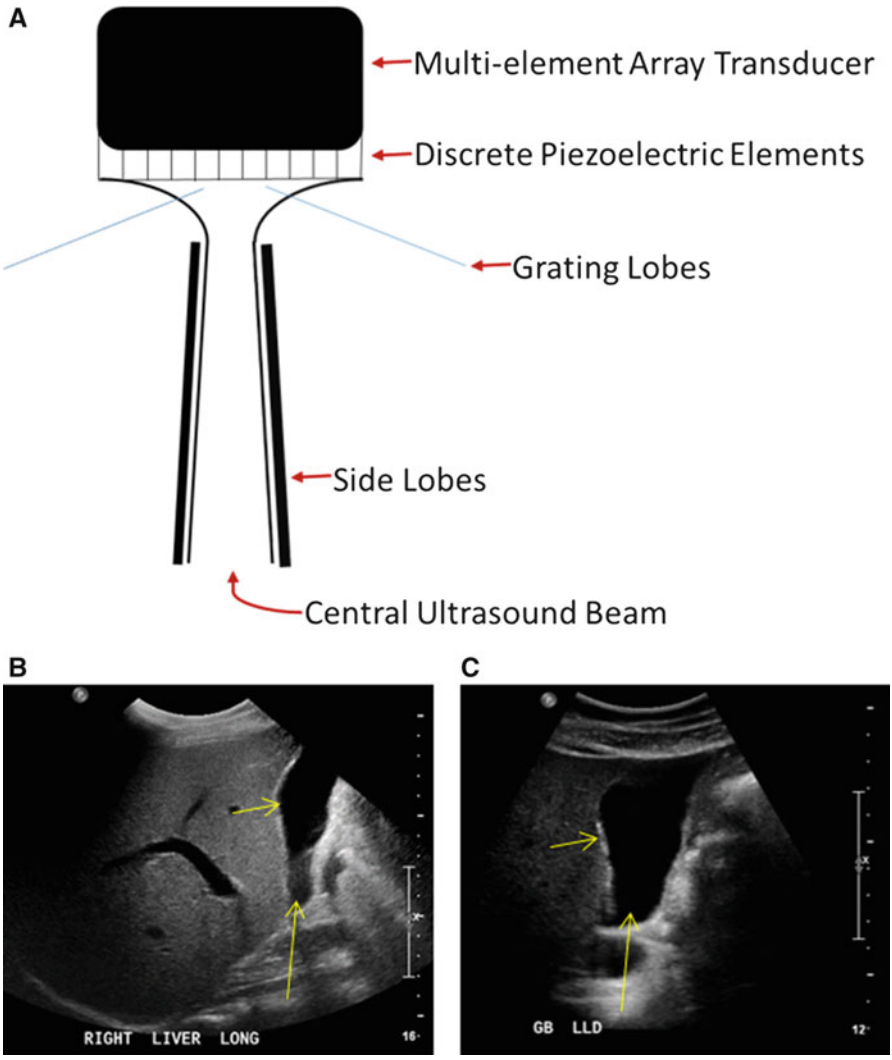

Fig. 12.22 *Side lobe and grating lobe artifacts.* (**a**) This schematic demonstrates where the side lobe echoes and grating lobe echoes are generated with respect to the ultrasound beam and the multielement transducer. The side lobe echoes radiate off-axis from the ultrasound beam, while the grating lobe echoes are generated at large angles to the transducer surface. (**b**) This grayscale image details the gallbladder (*small arrow*) within the periphery of the ultrasound image volume. The image suggests that there is layered echogenicity (*large arrow*) within the gallbladder, otherwise called sludge. (**c**) This dedicated image displays the gallbladder (*small arrow*) within the center of the ultrasound imaging volume. This dedicated image of the gallbladder illustrates that there is in fact no sludge (*arrow*) within its lumen, and the appearance of sludge within image B was attributable to a side lobe artifact or so-called pseudosludge

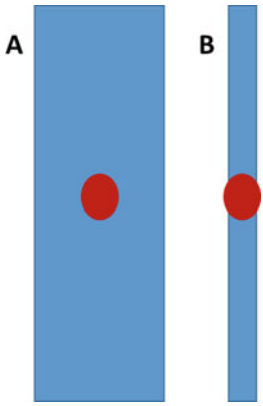

Fig. 12.23 *Partial volume averaging*. (**a**) Slice thickness greater than the imaged object results in averaging of the object's signal within the volume slice. This causes loss of signal and partial volume averaging. (**b**) Slice thickness smaller than the imaged object provides for improved axial spatial resolution

of the perceptibly smooth surface of the multi-array transducer surface by a collection of many closely assembled and discrete piezoelectric elements. This misdirected low-energy signal can produce ghost images of off-axis objects which are highly reflective within the image's central field of view (Fig. 12.22).

Grating lobe artifacts can be reduced by creating multielement array transducers that have the individual piezoelectric elements more tightly packed together with less intervening space.

12.7.3.4 Slice Thickness

An ultrasound beam possesses a finite thickness. The width of this slice thickness varies with distance from the transducer surface where it is greatest close to the transducer surface, most narrow at the focal distance, and progressively increasing with distance from the focal distance. A narrow image slice thickness provides for improved axial resolution. If an object is much smaller than the slice thickness, the signal from the object will be averaged within the slice volume, resulting in signal loss and partial volume averaging (Fig. 12.23).

12.7.3.5 Tissue Vibration

Tissue vibration is an artifact that arises when flow within a vessel is markedly disturbed from its normal developed flow pattern. This artifact emerges in vessels which are markedly narrowed at a focal stenosis with the creation of a vortical or swirling flow pattern downstream of the stenosis (Fig. 12.24). This disturbed flow with its separated or vortical pattern will create pressure fluctuations within the vessel lumen that will subsequently cause the vessel wall to resonate. Like all resonating structures discussed in this chapter, this resonance will generate a sound wave. Since the entire circumference of the vessel will vibrate, sound waves will emanate radially from the vessel. This radial emanation of low-amplitude sound

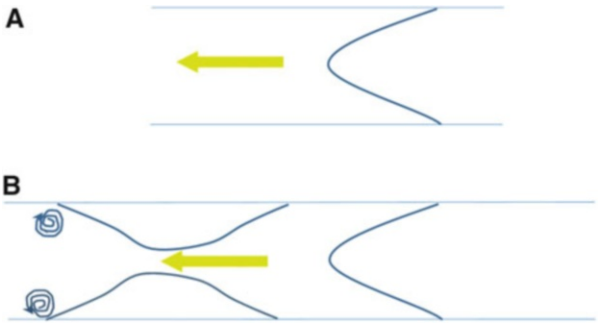

Fig. 12.24 *Vibration artifact*. As the blood travels through a stenotic area, the flow profile is disrupted from a developed parabolic description (**a**) to a separated waveform with areas of vortical flow (**b**)

waves will generate Doppler noise or a mixture of Doppler signal centered around the vessel. While the tissue vibration does create an artifact, the recognition of this artifact represents an important diagnostic clue for high-grade stensoses such as in the carotid arteries.

12.7.3.6 Speed Displacement

The speed of displacement artifact introduces a small element of error in ultrasound estimates of range and distance. This artifact results from the variation of the speed of sound in soft tissue (c_{fat} is equal to 1450 m/sec, $c_{\text{soft tissue}}$ is equal to 1540 m/sec) as opposed to the assumption that the speed of sound remains constant. This artifact can cause edges to be slightly mapped outward and introduce up to 6% error (Kremkau and Taylor 1986; Keogh and Cooperberg 2001).

12.8 Bioeffects of Ultrasound Imaging

Ultrasound imaging has been widely considered safe with negligible safety concerns. Unlike plain films and CT imaging, there is no associated radiation. For years, ultrasound has been utilized for obstetric imaging of pregnant patients and their babies with no reported adverse effects (Fig. 12.25). Within the published literature, there is no report of significant detrimental effects of ultrasound either on the patient or the sonographer.

Ultrasound generates images by observing the interaction of the body with sound energy. Anytime that energy is transmitted into the body, there exists the possibility of adverse effects such as tissue heating. Thermal deposition or tissue heating happens when transmitted sound energy is absorbed by tissue and converted to heat.

The amount of energy transmitted by ultrasound is reflected by the intensity value. Intensity is defined by the amount of energy per unit time that is transmitted through a unit area. Alternatively, intensity can be described as the power per unit area and is measured in terms of Watts/cm^2.

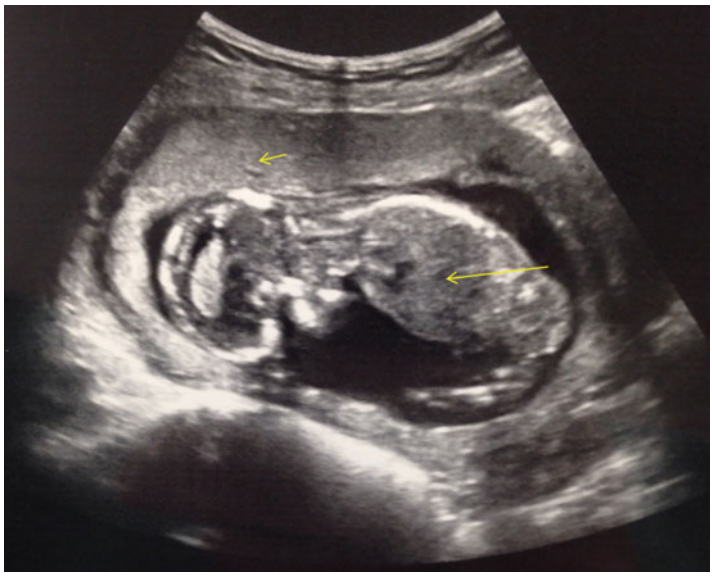

Fig. 12.25 *Obstetric ultrasound image*. Grayscale B-mode ultrasound image of a 12.5-week fetus (*long arrow*). The placenta (*short arrow*) is along the anterior surface of the uterus

All ultrasound equipment is evaluated and certified by the US Food and Drug Administration (FDA). The FDA has determined that there are no significant biological effects for diagnostic grayscale imaging obtained with ultrasound intensity transmitted below 100 mW/cm^2 or for Doppler imaging acquired with ultrasound intensity emitted below 1 W/cm^2. When imaging patients for diagnostic purposes, the intensity values are kept well below these threshold levels. Conventional intensity values in medical imaging range from 1 to 10 mW/cm^2.

Although ultrasound has long been considered safe with minimal side effects, this imaging tool, and for that matter all of imaging, should still be reserved for patients that will directly benefit from the acquired imaging information. When generating images, information should be obtained with the smallest amount of energy being transmitted into the patient. This approach reflects the ALARA principle or imaging with energy *as low as reasonably achievable* to obtain useful diagnostic information.

12.9 Advancements in Ultrasound

12.9.1 Harmonic Imaging

As with all of medical imaging, there is continuous advancement within the field. Most modern-day ultrasound machines acquire information using harmonic imaging. Up to this point, we have described a process where the images are generated

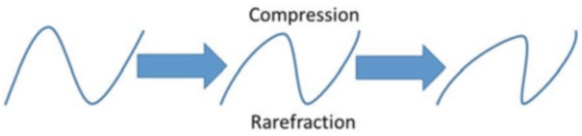

Fig. 12.26 *Harmonic frequency generation.* Harmonic frequencies are generated by the distortion of the transmitted ultrasound beam. The positive pressure amplitude portions of the wave (*compression*) travel faster than the negative pressure amplitude portions of the wave (*rarefaction*)

from sound frequencies that are identical to the initial transmitted ultrasound pulse. When ultrasound energy is transmitted into the body, its interaction with adjacent tissue produces sound waves with frequencies that are integer multiples of the initial transmitted or fundamental frequency (f_0). The harmonic frequencies originate when the ultrasound energy interacts with tissue and the positive pressure amplitude portions of the wave (compressions) travel faster than the negative pressure amplitude portions of the wave (rarefactions). This interaction results in distortion of the wave (Fig. 12.26). As the sound wave travels farther into the tissue, this nonlinear distortion of the wave increases in extent. The higher-order harmonics will be weakened in strength from the fundamental harmonic, but since they will only travel the return distance to the transducer, their signal strength remains relatively strong. Additionally, since the harmonic signal avoided the fundamental frequency's initial interaction with the overlying skin, subcutaneous tissue, and body wall, its signal is less contaminated by noise or the clutter commonly encountered near the ultrasound transducer. This helps to augment the signal to noise ratio (SNR) of the returned signal.

When the harmonics return to the ultrasound transducer, a filter is employed to isolate the higher-order harmonic information. Generally, the first harmonic (f_1) or twice the fundamental frequency is isolated for imaging. Harmonic imaging is best suited for applications such as abdominal imaging where a lower-frequency transducer probe is employed (3.5–5 MHz), and the harmonic imaging allows for evaluation with the higher-frequency harmonics which are less contaminated by the noise originating close to the probe (Fig. 12.27).

12.9.2 Ultrasound Contrast Agents

Ultrasound contrast agents have gained growing attention in recent years. While use within the United States is limited to echocardiography (functional ultrasound imaging of the heart), ultrasound contrast agents are used with far greater application in Canada and Europe for vascular imaging and perfusion imaging of abdominal masses, particularly within the liver. The ultrasound contrast agents are microbubbles, measuring between 3 and 6 μm in diameter, which contain either air, nitrogen, or perfluorocarbons. The encapsulation material, typically albumin, is

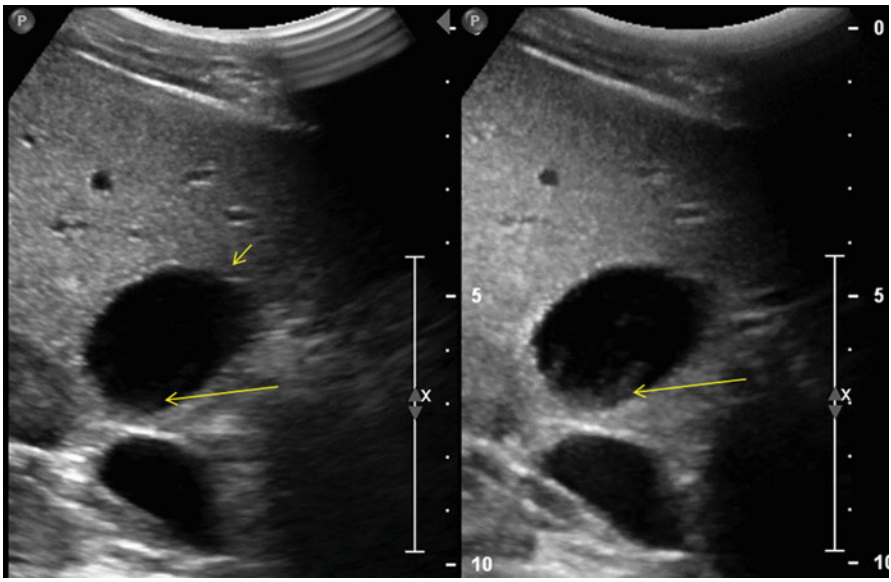

Fig. 12.27 *Harmonic imaging*. The image on the left demonstrates conventional fundamental frequency imaging of the gallbladder (*short arrow*). Within this image, there is some suggestion of echogenic material which is dependently layered (*long arrow*). The image on the right illustrates harmonic imaging of the gallbladder. The dependently layered echogenic material is more conspicuous (*long arrow*) and is consistent for a small amount of sludge

designed to contain the gas within the microbubble until the agent has reached the target tissue to be imaged. An image is generated due to the large difference in acoustic impedance between the ultrasound contrast agent and the surrounding tissue. For vascular imaging, the microbubbles increase the scatter signal from the blood, providing for far greater conspicuity of Doppler signal from flowing blood. Since the microbubbles contain compressible gas, their interaction with the incident ultrasound energy produces oscillations. These oscillations generate higher-order harmonics with higher signal amplitude than the harmonics generated by soft tissue. These higher amplitude harmonics are then detected by a technique called pulse inversion harmonic imaging. With pulse inversion harmonic imaging, the information from the surrounding soft tissue is removed which isolates the signal from the contrast agent. This technique improves the ability to observe tissue perfusion. This is critically important when evaluating masses within the liver and attempting to observe their dynamic perfusion characteristics (Bushberg et al. 2002; Weng et al. 1997; Balen et al. 1994).

12.10 Compound Imaging

This is a relatively new technique which can be performed in two different approaches: (1) frequency compounding and (2) spatial compounding. With compound imaging, multiple imaging frames are acquired either at different frequencies (frequency compounding) or at different angles (spatial compounding). This information is combined into a single multifrequency or multi-angle image which demonstrates enhanced image contrast. This imaging technique has the ability to improve image conspicuity so that pathology that was otherwise inapparent can now be visualized and evaluated.

12.11 Three-Dimensional Imaging

Three-dimensional (3D) images are generated from a series of contiguous two-dimensional images acquired from a volume of tissue. Using a stack of 2D images, data reordering can be used to create a 3D image. The 3D image is displayed using either maximum intensity projection (MIP), multiplanar reformatting (MPR) (Fig. 12.28), or surface rendering (most frequently used for displaying facial structures in obstetric imaging).

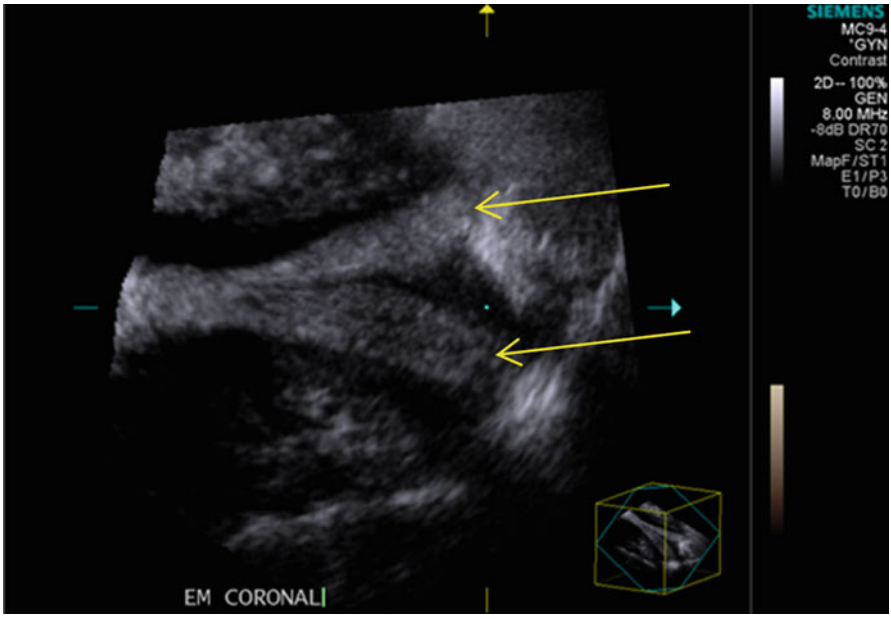

Fig. 12.28 *Three-dimensional ultrasound imaging*. Multi-planar reformatting of the uterus demonstrating the two uterine horns (*arrows*) in a didelphys uterine malformation

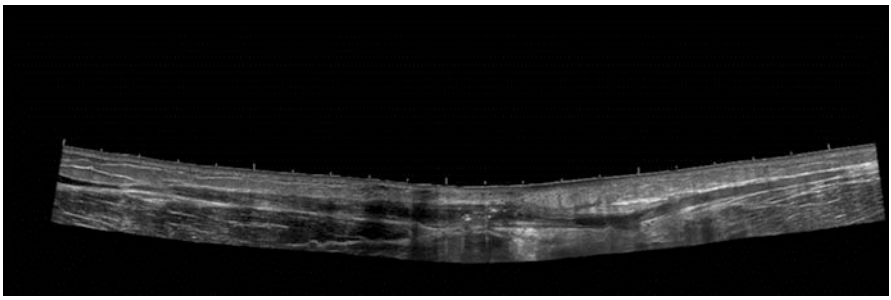

Fig. 12.29 *Extended-field-of-view imaging*. This image represents an extended field of view of the cephalic vein (a small superficial vein) within the left forearm

12.12 Extended Field of View

One recognized constraint of ultrasound imaging is how its field of view is limited to what the transducer can visualize within its plane of interrogation. For visualizing objects that extend over more than one field of view, this constraint can make image interpretation by the radiologist more difficult. New ultrasound machines have the ability to generate a panoramic view in real time which extends beyond the limits of one single field of view. New image processing software provides image registration of probe position which can lead to the synthesis of the extended-field-of-view image (Fig. 12.29) (Weng et al. 1997).

12.13 Conclusions

Ultrasound represents a noninvasive, radiation-free technique that provides imaging in real time. With continued advancements in hardware design and image post-processing techniques, the scope of ultrasound application continues to expand. Ultrasound has always been able to provide functional information through color Doppler imaging and real-time imaging of moving structures such as the heart. With further development of microbubble contrast agents, ultrasound imaging has only just started to investigate the growing field of dynamic perfusion imaging. With the mounting emphasis to develop techniques that are accurate and less expensive, ultrasound is assured to maintain an eminent role in medical imaging.

Questions

1. If a forearm muscle is evaluated with a 10 MHz linear array transducer, what is the wavelength (λ) of the transmitted ultrasound pulse? The velocity of sound in muscle is 1585 m/sec.
2. An ultrasound beam passes through the liver, and its intensity is attenuated by 70%. By how many dB has the intensity decreased?

3. Describe the four different interactions that can occur when sound encounters an acoustic interface.
4. For an incident sound intensity of 100 mW/cm^2, calculate the transmitted sound intensity as the pulse travels from fat to muscle. Z_{fat} equals 1.38 Rayl, and Z_{muscle} equals 1.70 Rayl.
5. Sound passes from retroperitoneal fat into the kidney. The initial angle of incidence, Θ_i, is equal to 45°. What is the angle of refraction, Θ_t? The speed of sound in fat is 1450 m/sec, while the speed of sound in soft tissue is 1540 m/sec.
6. For a transducer with an element length of 7 mm, calculate the focal distance for transmission in soft tissue at a frequency of 5 MHz and 10 MHz. The speed of sound in soft tissue is 1540 m/sec.
7. For a transducer with an element length of 8 mm, calculate the angle of ultrasound beam divergence (Θ_{div}) within the far field for transmission in soft tissue with a frequency of 5 MHz. The speed of sound in soft tissue is 1540 m/sec.
8. Ultrasound spatial resolution is described in three different dimensions. List them.
9. A 5 MHz phased array transducer is used to transmit a pulse echo with 5 cycles. For transmission in soft tissue with a speed of sound of 1540 m/sec, calculate the spatial pulse length. What is the axial resolution or the minimum distance that can separate two adjacent objects along the axial direction of the ultrasound pulse?
10. A. What is the type of echo display mode that is used to generate a grayscale image of the liver? B. What is the type of echo display mode that is used to estimate the heart rate of a fetus?
11. Using a 5 MHz transducer, calculate the frequency shift for blood moving at 100 cm/sec with the speed of sound measuring 1540 m/sec and θ, the angle between the transmitted sound and the direction of blood flow, equal to 45°.

Answers

1. 0.159 mm.
2. The intensity has decreased by −5.23 dB.
3. Reflection, refraction, scatter, and absorption.
4. 98.92 mW/cm^2.
5. 48.7°.
6. At 5 MHz the focal distance equals 39.8 mm, while at 10 MHz the focal distance equals 79.6 mm.
7. 2.69°.
8. Axial resolution, lateral resolution, and azimuthal resolution.
9. The spatial pulse length equals 1.54 mm. The axial resolution equals 0.77 mm.
10. A. B-mode. B. M-mode.
11. 4.591 kHz.

References

Balen FG, Allen CM, Lees WR (1994) Ultrasound contrast agents. Clin Radiol 49(2):77–82
Bigelow TA, Church CC, Sandstrom K et al (2011) The thermal index: its strengths, weaknesses, and proposed improvements. J Ultrasound Med Off J Am Inst Ultrasound Med 30(5):714–734
Bude RO, Rubin JM (1996) Power Doppler sonography. Radiology 200(1):21–23
Bushberg J, Seibert J, Leidholdt E et al (2002) The Essential Physics of Medical Imaging, 2nd edn. LWW, Philadelphia
Goldstein A (1993) Overview of the physics of US. Radiogr Rev Publ Radiol Soc North Am Inc 13 (3):701–704
Hendrick WR, Hykes DL, Starchman DE (1995) Ultrasound physics and instrumentation, 3rd edn. Mosby, St Louis
Keogh CF, Cooperberg PL (2001) Is it real or is it an artifact. Ultrasound Q 17(4):201–210
Kremkau FW (1993) Multiple-element transducers. Radiogr Rev Publ Radiol Soc North Am Inc 13(5):1163–1176
Kremkau FW (1998) Diagnostic ultrasound: principles and instruments, 5th edn. WB Saunders, Philadelphia
Kremkau FW, Taylor KJ (1986) Artifacts in ultrasound imaging. J Ultrasound Med Off J Am Inst Ultrasound Med 5(4):227–237
Rubin JM (1994) Spectral Doppler US. Radiogr Rev Publ Radiol Soc North Am Inc 14 (1):139–150
Weng L, Tirumalai AP, Lowery CM et al (1997) US extended-field-of-view imaging technology. Radiology 203(3):877–880
Zagzebski J (1996) Essentials of ultrasound physics. Mosby, St. Louis
Ziskin MC (1993) Fundamental physics of ultrasound and its propagation in tissue. Radiogr Rev Publ Radiol Soc North Am Inc 13(3):705–709